nature portfolio

Peer Review File

Optical access of spin-polarized excited states in Cs(PbMgZnCd)Br3 nanocrystals

Corresponding Author: Professor Chuang Zhang

This file contains all reviewer reports in order by version, followed by all author rebuttals in order by version.

Version 0:

Reviewer comments:

Reviewer #1

(Remarks to the Author)
In this manuscript, Zhang et al. reported the synthesis of high-entropy Cs(PbMgZnCd)Br3 nanocrystals and observed a reasonably long spin polarized excited states at room temperature. The authors discovered that the high-entropy structure can both facilitate the radiative recombination rate and prolong the spin relaxation time. On this basis, they show optical Hanle effect for both photoluminescence and amplified spontaneous emission from high-entropy perovskite nanocrystals, which can used for the robust optical access of spin-polarized excited states towards potential opto-spintronic applications. The exploration of spin-related properties in high-entropy perovskite materials is interesting. The experimental results suggested the formation of high-entropy structure can tune photo-physical and spin-physical parameters, which is very valuable to the field of spintronics. Overall, the manuscript is in good shape. I have several questions and comments for the authors to address before this manuscript can be accepted.

1. How are the stability and reproducibility of the high-entropy nanocrystals? I assume the high-entropy sample is more environmental sensitive to the pristine CsPbBr3 nanocrystals. Also, statistics on sample batches should be provided.
2. Why the series of Mg, Zn, and Cd as non-Pb metals in the high-entropy structure? Was any consideration given to the ionic size of non-Pb metals?
3. Only $[PbBr6]^{4-}$ is considered in the radiative recombination of high-entropy nanocrystals. The authors provide theoretical calculations to explain why the non-Pb $[MBr6]^{4-}$ is not emissive. Can they provide some control experimental results to further clarify the roles of non-Pb metals in the structural and optical properties.
4. In Fig. 4a,b, the authors explained the extended lifetime due to lattice distortion triggered enhanced Rashba splitting. The authors stated the energy splitting ER rises from 0.068 eV for CsPbBr3 to 0.274 eV in high entropy alloy. With thermal energy only 0.059 eV at room temperature, how can spin up and spin down carriers overcome this 0.274 eV activation barrier? There can be potential other pathways but not just Rashba splitting that can explain the trend. I suggest the authors to further discuss the spin-flip mechanism.
5. In another note, Rashba splitting generate a difference in k vector basically changing a direct gap into an indirect gap. In this way, one would expect an elongated charge recombination lifetime and suppressed PL emission. In the experiment, an opposite trend is observed where high entropy alloy decreases the recombination lifetime with higher PL quantum yield. The authors should probably also explain this point on how the larger Rashba splitting can generate shorter recombination lifetime.
6. Amplified spontaneous emission from CsPbBr3 nanocrystals should also be measured. Can the circular polarization of ASE be observed at room temperature for CsPbBr3 nanocrystals?
7. For the results of temperature dependence (for instance, Fig. 5d and 5e), the authors attribute it to the suppression of phonon-assisted thermal perturbations. Is there any contribution from the structural change or phase transition at cryogenic temperatures?
8. Minor issue: it is better to change PPL into PASE in Fig. 6b and 6c.
9. Another minor issue, the authors should provide photoinduced spectra for left and right circularly polarized pump to show where the kinetics are taken for better comparison.

Reviewer #2

(Remarks to the Author)

The major advance reported in the paper
This study marks an exciting breakthrough in the field of opto-spintronic halide perovskites by showing, for the first time, that spin-polarized excited states (SPESs) can be observed at room temperature. Until now, such studies were only possible at cryogenic temperatures because of fast spin relaxation and poor photoluminescence efficiency under ambient conditions. The authors overcame this challenge by using high-entropy Cs(PbMgZnCd)Br3 perovskites, where the presence of multiple metal cations creates strong lattice distortions in the $[PbBr_6]^{4-}$ framework. These distortions enhance Rashba spin–orbit coupling, allowing the excitons to maintain their spin polarization for longer times. As a result, circularly polarized light could be used to probe SPESs even at room temperature. This is a major step forward, as it brings the study of spin phenomena closer to real-world device applications. Beyond the immediate results, the work highlights how high-entropy design can be a powerful approach to tune spin dynamics and structural properties in perovskites, paving the way for the development of next-generation room-temperature opto-spintronic materials.

Technical suggestion:
•Frequent references to multiple figures within the same paragraph can disrupt the flow of reading and make it difficult for readers to maintain focus. Reducing such repetition and integrating figure references more strategically would improve clarity and enhance the overall readability of the article.
•The study mentions the spatial distribution of Pb, Mg, Zn, and Cd in the nanocrystals but does not provide detailed statistical analysis or quantitative data on the uniformity of doping. Variations in doping levels could impact the reproducibility and performance of the material. Quantitative data obtained by SEM-EDS or TEM-EDS can be included.
•Providing a detailed deeper insight into the mechanisms that prevent non-radiative losses responsible for a high PLQY (~98.5%) for Cs(PbMgZnCd)Br3 would be beneficial.
•In Figure 5, ensuring that the caption and the figure appear on the same page would improve visual appearance.
•The overall text alignment and formatting could be enhanced to improve readability and coherence. It is recommended to ensure consistent font size, margins, and spacing throughout the manuscript.
•Including a discussion on specific future research directions would help contextualize the broader impact of the study and guide subsequent investigations in the field.

Reviewer #3

(Remarks to the Author)
This work reports a compelling study of spin-dependent excitonic properties in a high-entropy material, Cs(PbMgZnCd)Br3 nanocrystals. An exceedingly long spin relaxation time up to ~60ps is realized, accompanied by a short radiative recombination (~3.4ns), leading to possible spin control of spin-polarized excitonic states at room temperature. This study is centered on an equation describing the correlation between the circular polarization of emission and a ratio of spin relaxation time to radiative recombination time, as shown on page 9. To increase the spin relaxation time while reducing the radiative time, this work aimed to tailor the spin-dependent properties of nanocrystals by inducing substitutional elements into CsPbBr3 nanocrystals. The high-entropy structure of Cs(PbMgZnCd)Br3 induces a large Rashba splitting state that can significantly increase the spin relaxation time, while the excitonic confinement reduces the radiative time. The large circular polarization is demonstrated by circularly polarized TA and optical Hanle measurements. Another compelling result in this work is to utilize the short radiative time during the ASE process, resulting in a large circular polarized ASE up to 26% at room temperature. Remarkably, this work also reported the first optical Hanle effect of circular polarized ASE, fully demonstrating the optical access of spin-polarized excitonic state under a magnetic field. This is a complete work highlighting the great potential of circularly polarized PL/ASE for spin control. The manuscript is well-organized, and the data quality is marvelous. Thus, I would recommend the publication of this work in Nature Communications after the following comments are fully addressed.

[1] What's the key rationale to choose a composition including Mg, Zn, and Cr? I understand the current composition can induce excitonic confinement. However, if a large Rashba splitting requires strong SOC, should the Pb be replaced by higher SOC elements instead of lower ones?

[2] The claimed large Rashba spin splitting needs to be validated. What's the value of the Rashba parameter compared to that in the conventional CsPbBr NCs? On page 8, the calculations show the energy splitting and momentum shift in two compounds. From these values, the calculated Rashba parameter in CsPbBr (1.28eVA) is larger than that in the Cs(PbMgZnCd)Br3 (0.89 eVA). This contradicts the main statement about the increase in spin relaxation time due to the formation of a larger Rashba state. In addition, do authors conduct any CPGE measurement to validate the spin-momentum correlation? Only the DFT calculation does not adequately prove the presence of the Rashba splitting.

[3] Could authors provide a table to compare the obtained tau_s in other compounds from literature reports? Is this value of 34ps adequately long?

[4] It is stated that the D'yakonov-Perel mechanism is responsible for the larger spin relaxation time in the presence of Rashba splitting. The Rashba splitting does not guarantee the DP model. Have the authors conducted a plot of tau_s as a function of tau_p to validate the DP mechanism?

Minor issues in SI:
[5] What are the red and dark plots in Fig. S7? Please update the caption accordingly.
[6] Is there any phase transition that can cause a blueshift of PL as temperature increases, as shown in Fig. S9?
[7] Fig. S8 and Fig. S13 are band structures for the same CsPbBr3 at different k vectors. Is there no Rashba spin splitting

between gamma-z, gamma-Y, etc?
[8] Fig.S26 indicates this is ‘laser emission’. Would this be ASE emission only?

Version 1:

Reviewer comments:

Reviewer #1

(Remarks to the Author)
The author have addressed most of my concerns. I just have one comment related to my previous comment 5 that Rashba splitting should reduce PL emission instead of enhancing it. The authors explained with quantum confinement effect and exciton Bohr radius. This may still not be the cause of enhanced PL emission as these two effects does not directly influence k-vector which governs the PL emission efficiency. I think maybe this article could help the authors to explain the Rashba trend that the k-vector tuning could help PL emission. ACS Nano 2025, 19, 35, 31331–31339. I am wondering if the quantum dots the authors synthesized could experience the same type of k-vector aligning. Apart from this point, I think this paper is in good shape to be published.

Reviewer #3

(Remarks to the Author)
The authors have carefully addressed most of the comments; however, I remain unsatisfied with one specific response.

In my previous comment (#2), I suggested conducting CPGE measurements to validate the presence of the Rashba splitting in Cs(PbMgZnCd)Br3, as this is the only viable characterization approach to directly probe the Rashba state. However, the device geometry utilized by the authors (Fig. R12) represents a typical circularly polarized photodetector configuration rather than a proper CPGE setup.
For valid CPGE measurements, the detected photocurrent must be transverse to the plane of the incident laser due to the well-established spin-momentum locking at the Rashba state. Furthermore, the authors need to perform laser incidence angular-dependent measurements of the CPGE photocurrent. Specifically, they need to demonstrate that the sign of the photocurrent inverts when the angle of laser incidence is reversed. Without this angular dependence and the correct transverse geometry, the results cannot be definitively attributed to the Rashba effect.

Version 2:

Reviewer comments:

Reviewer #1

(Remarks to the Author)
The authors have addressed all my comments. The paper can now be accepted.

Reviewer #3

(Remarks to the Author)
The authors have addressed my concern about CPGE measurements. Now, I recommend publishing this work as is.

Reviewer #4

(Remarks to the Author)
This work reports the synthesis and optical characterization of high-entropy perovskite colloidal nanocrystals, Cs(PbMgZnCd)Br3, in which partial substitution of Pb2+ with a mixture of Mg2+, Zn2+, and Cd2+ creates isolated and distorted [PbBr6]4- luminescent domains. The authors demonstrate that this structural engineering simultaneously shortens the radiative lifetime (τ_R ~ 3.4 ns) via quantum confinement and prolongs the spin relaxation time (τ_S ~ 59.8 ps) via enhanced Rashba spin splitting, enabling optical write-in and read-out of spin-polarized excited states at room temperature with a circular polarization up to 25.8% in amplified spontaneous emission.

1. The authors propose that high-entropy doping spatially partitions the [PbBr6]4- framework into isolated domains smaller than the exciton Bohr radius, thereby inducing quantum confinement. However, direct and quantitative evidence regarding the actual size, size distribution, and the degree of electronic coupling between these domains is lacking. The current evidence primarily relies on HAADF-STEM contrast analysis and the observation of a PL blue-shift, which are indirect indicators. It is recommended that the authors supplement the study with pair distribution functon(PDF) analysis or small-angle X-ray scattering (SAXS) to provide a more quantitative description of the spatial extent and isolation of the [PbBr6]4- domains. If such data are unavailable, the speculative nature and associated uncertainties of this structural model should be explicitly addressed in the discussion.

2. The authors note that the temperature dependence of the spin relaxation time cannot be adequately fitted by a single D'yakonov-Perel (DP) or Elliott-Yafet (EY) mechanism across the entire temperature range and suggest a combination of both. However, a detailed analysis of the underlying physical origins for this behavior is missing, and potential contributing factors such as exciton localization, surface states, or defect-assisted scattering are not discussed. Furthermore, details of the fitting attempts shown in Figure S28 are insufficient, making it difficult for the reader to assess the extent of deviation from each model. The authors should provide a more comprehensive analysis, at minimum identifying the dominant mechanism in the low- and high-temperature regimes and discussing how the specific lattice distortions in the high-entropy structure modify the conventional theoretical picture of spin relaxation.

3. The fitting of the optical Hanle effect relies on the effective Landé g-factor and the effective lifetime T. While the authors assert that $T \approx \tau_S$ (based on $\tau_S \ll \tau_R$), the explicit g-factor value used in the fitting is not provided, nor is it independently verified. For a high-entropy perovskite with strong spin–orbit coupling, the g-factor may differ from that of pristine CsPbBr3 and could exhibit anisotropy. To ensure the reliability of the extracted τ_S values, the authors should clearly state the fitting parameters employed. Ideally, an independent magneto-optical measurement (e.g., magnetic circular dichroism or magneto-PL) should be performed to calibrate the exciton g-factor. The current simplified treatment of the Hanle curve fitting warrants further justification.

4. A central conclusion of this work is the unique advantage of synergistic high-entropy doping (simultaneous incorporation of Mg, Zn, and Cd) in enhancing lattice distortion and prolonging τ_S. However, the experimental comparison is limited solely to undoped CsPbBr3 versus Cs(PbMgZnCd)Br3. Crucial control experiments involving single-metal doping (e.g., CsPb1-xMgxBr3) or binary doping at comparable total substitution levels are absent. While the authors note the difficulty of high-level single-metal doping, control samples prepared within the achievable doping limits would be highly valuable to confirm the necessity of the high-entropy configuration and to rule out simple additive effects of the individual dopants. The inclusion of such comparative data, or an extended discussion comparing the present results with existing literature on single-dopant τ_S values, would substantially strengthen the manuscript's claims.

5. The authors demonstrate a high degree of circular polarization (~25.8%) in amplified spontaneous emission (ASE) at room temperature and showcase multi-level optical write-in/read-out. This is a highlight of the work. However, the verification of the temporal and thermal stability of this polarized ASE, as well as its reproducibility, is rather limited (only briefly mentioned in relation to Figure S34). Furthermore, the high polarization is achieved under femtosecond pulsed excitation; it remains unclear whether similar performance can be sustained under continuous-wave optical pumping or, ultimately, electrical injection, which is more relevant for practical device applications. The authors are encouraged to provide additional data on the evolution of ASE circular polarization over extended operation times (minutes to hours) and thermal cycling. A preliminary discussion or outlook regarding the potential performance under continuous excitation would enhance the technological relevance of these findings.

Version 3:

Reviewer comments:

Reviewer #4

(Remarks to the Author)
The authors have addressed all my comments. The paper can now be accepted.

Response to Reviewers' Comments (NCOMMS-25-80800)

Reviewer #1

In this manuscript, Zhang et al. reported the synthesis of high-entropy $Cs(PbMgZnCd)Br_3$ nanocrystals and observed a reasonably long spin polarized excited states at room temperature. The authors discovered that the high-entropy structure can both facilitate the radiative recombination rate and prolong the spin relaxation time. On this basis, they show optical Hanle effect for both photoluminescence and amplified spontaneous emission from high-entropy perovskite nanocrystals, which can used for the robust optical access of spin-polarized excited states towards potential opto-spintronic applications.

The exploration of spin-related properties in high-entropy perovskite materials is interesting. The experimental results suggested the formation of high-entropy structure can tune photo-physical and spin-physical parameters, which is very valuable to the field of spintronics. Overall, the manuscript is in good shape. I have several questions and comments for the authors to address before this manuscript can be accepted.

Our Response: We sincerely appreciate Reviewer #1 for the very positive evaluation and his/her time and efforts in examining our work. In the following, we have provided detailed responses to Reviewer #1's comments, and the main text and Supplementary Information have been revised accordingly.

1. How are the stability and reproducibility of the high-entropy nanocrystals? I assume the high-entropy sample is more environmental sensitive to the pristine $CsPbBr_3$ nanocrystals. Also, statistics on sample batches should be provided.

Our Response: In the high-entropy nanocrystals, the perovskite lattice is stabilized by the configurational entropy introduced by the doping of multiple metal cations. The high-entropy structure is therefore highly stable compared with the conventional single-metal doping perovskites at high doping levels. Note that the structural collapse would

eventually occur during the decomposition of $CsPbBr_3$ perovskites under ambient conditions (oxygen and water). To evaluate the environmental stability, we monitored the PL spectra of thin films of $CsPbBr_3$ and $Cs(PbMgZnCd)Br_3$ nanocrystals under ambient conditions for 10 days, as shown in **Figure R1**. The two samples show comparable decay curves, and the decomposition of $Cs(PbMgZnCd)Br_3$ appears slightly more sensitive to moisture/oxygen than that of $CsPbBr_3$ over extended periods.

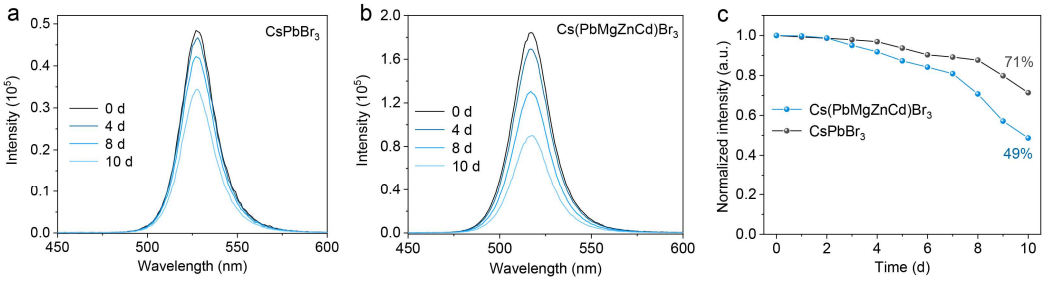

Figure R1. PL spectra of (a) $CsPbBr_3$ and (b) $Cs(PbMgZnCd)Br_3$ nanocrystals recorded under ambient conditions over a period of 10 days. (c) PL intensity as a function of storage time for $CsPbBr_3$ and $Cs(PbMgZnCd)Br_3$ nanocrystals.

For the reproducibility of high-entropy nanocrystals, we have provided statistics from sample batches according to Reviewer #1's comments. As shown in **Figure R2a**, the statistical analysis on SEM-EDS results of 20 parallel samples shows that they have very narrow distributions on elemental compositions (Pb ~ 30%, Mg ~ 20%, Zn ~ 24%, and Cd ~ 26%). It indicates that the product is a thermodynamically favored outcome governed by the interplay between configurational entropy and the solubility of the corresponding MBr_2 salts during the ion-exchange process. We have also analyzed the PL peak wavelengths for these samples (**Figure R2b**), which is related to exciton confinement determined by the distribution of Pb and non-Pb metal ions in the perovskite structure. The very narrow distribution centered at ~515 nm verifies the good reproducibility of as-prepared high-entropy nanocrystals.

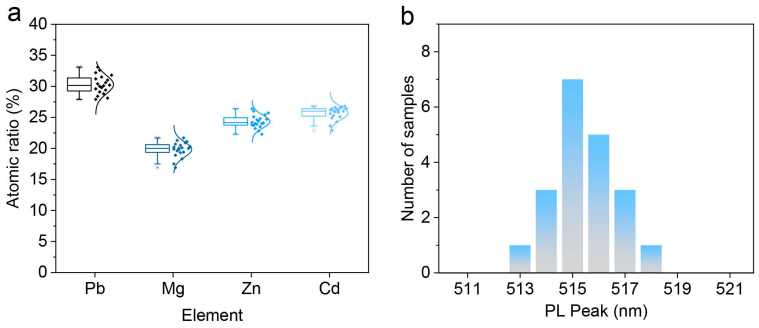

Figure R2. Statistical analysis of 20 parallel samples of Cs(PbMgZnCd)Br_3: (a) the distributions of Pb, Mg, Zn, and Cd atomic ratios obtained from SEM-EDS measurements; (b) the distributions of PL peak wavelengths.

Accordingly, we have supplemented **Figure R1** and **Figure R2** as **Figure S11** and **Figure S4/S10**, respectively. The discussions have also been added in the main text (page 4, 6) as well as Supplementary Information.

2. Why the series of Mg, Zn, and Cd as non-Pb metals in the high-entropy structure? Was any consideration given to the ionic size of non-Pb metals?

Our Response: In the rigid $CsPbBr_3$ lattice, the replacement of Pb with smaller B-site cations allows for a strong lattice distortion. Meanwhile, the compressed $[MBr_6]^{4-}$ octahedra usually have a larger band gap and thus benefit the exciton localization in the $[PbBr_6]^{4-}$ octahedra. However, the Goldschmidt tolerance factor has to be carefully considered for single-metal doping in perovskite structures (added as 28, *Sci. Adv.* **2019**, *5*, eaav0693). According to recent studies (ref. 23, *J. Am. Chem. Soc.* **2022**, *144*, 5864-5870), the high-entropy perovskites can overcome the above limitations and enable high-level multi-metal doping in the rigid lattice. For instance, the ionic sizes of Mg, Zn, Cd and Pb are 0.72, 0.74, 0.95 and 1.19 Å, respectively. The large mismatch in ionic sizes precludes high-level single-metal doping in perovskite structures, but a mixture of these non-Pb ions (Mg, Zn, Cd) can be simultaneously introduced in the high-entropy perovskite with both structural stability and lattice distortions.

Accordingly, the above discussions and related references have been added in the

main text (page 4) as well as Supplementary Information.

3. Only $[PbBr_6]^{4-}$ is considered in the radiative recombination of high-entropy nanocrystals. The authors provide theoretical calculations to explain why the non-Pb $[MBr_6]^{4-}$ is not emissive. Can they provide some control experimental results to further clarify the roles of non-Pb metals in the structural and optical properties.

Our Response: The sizes of M ions are all smaller than Pb^{2+} and the shorter M-Br bonds strengthen the orbital hybridization, pushing the $[MBr_6]^{4-}$-related states deep into the valence/conduction bands. Therefore, the $[MBr_6]^{4-}$ octahedra are not expected to contribute to band-edge emission, which is also supported by our PDOS (**Figure 3d**) analysis. Experimentally, no evidence of multiple types of emission centers is observed. For instance, the shape of emission spectrum is independent of the wavelength across the range of excitation band, while the excitation spectrum also remains the same for the entire emission band.

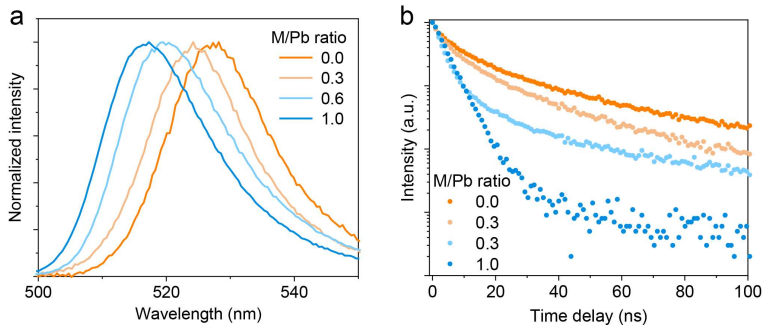

Figure R3. PL spectra (a) and PL decay dynamics (b) measured for the high-entropy LHPs with various M/Pb ratios.

The control experiments have been performed by gradually increasing the amount of Mg, Zn, and Cd (denoted as M) during ion exchange. The PL spectra (**Figure 3b** in the main text) and lifetimes of these control samples were measured to clarify the role of non-Pb metals, as shown in **Figure R3**. As the M/Pb ratio (M/Pb=1.0 means Mg:Zn:Cd:Pb=1:1:1:1 in the raw materials) increases, the PL peak shows a continuous blue shift accompanied by a gradual shortening of the PL lifetime. No secondary PL

band could be observed, which verifies that only $[PbBr_6]^{4-}$ octahedra are the emission centers while they are spatially separated by $[MBr_6]^{4-}$ units. The exciton confinement of isolated $[PbBr_6]^{4-}$ domains results in the blue shift of PL peaks and the facilitated radiative recombination upon the replacement of Pb with M ions.

Accordingly, we have supplemented **Figure R3** as **Figure S8**, and the discussions have also been added in the main text (page 6) as well as Supplementary Information.

4. In Fig. 4a,b, the authors explained the extended lifetime due to lattice distortion triggered enhanced Rashba splitting. The authors stated the energy splitting E_R rises from 0.068 eV for $CsPbBr_3$ to 0.274 eV in high entropy alloy. With thermal energy only 0.059 eV at room temperature, how can spin up and spin down carriers overcome this 0.274 eV activation barrier? There can be potential other pathways but not just Rashba splitting that can explain the trend. I suggest the authors to further discuss the spin-flip mechanism.

Our Response: We appreciate Reviewer #1 for his/her insightful comments. In the systems with the Rashba effect, the band splitting is characterized by both an energy scale (E_R) and a momentum offset (k_R, i.e., the k-space splitting), which together determine the spin texture of the band-edge states. We realize that Reviewer #1 is correct that spin relaxation is not simply governed by thermal energy over E_R; instead, it is typically controlled by the phonon-assisted spin relaxation pathways, which have been reported previously for $CsPbBr_3$ and other types of lead-halide perovskites (added as ref. 46, *J. Am. Chem. Soc.* **2024**, *146*, 12225-12232; added as ref. 47, *J. Phys. Chem. Lett.* **2025**, *16*, 5681-5686). For instance, Dyakonov-Perel (DP) type spin relaxation (spin dephasing) is caused by spin precession in a *k*-dependent spin-orbit field continuously randomized by phonon-induced momentum scattering; and Elliott-Yafet (EY) type spin relaxation (spin flips) occurs due to SOC-induced spin mixing of the electronic states during phonon scattering. In the high-entropy perovskites, the k-space splitting k_R increases by one order of magnitude (from 0.053 to 0.305 $Å^{-1}$), and therefore it can influence the above phonon-assisted spin relaxation processes.

In our studies, spin-polarized excited states are optically generated using circularly polarized excitation, and the circular polarization of photoluminescence is determined by the competition between radiative recombination (τ_R) and spin relaxation (τ_S). Experimentally, the temperature dependence of τ_S can be extracted from the optical Hanle effect measured at various temperatures, as shown in **Figure R4**. Notably, the experimental τ_S values as a function of T cannot be described by either the DP model or the EY model over the entire temperature range. It is more like a combination of DP and EY mechanisms, as well as contributions from the recombination/trapping and inhomogeneous broadening. Anyway, the larger k-space splitting associated with the enhanced Rashba effect is consistent with the slower spin depolarization observed in high-entropy perovskites. The momentum mismatch between spin-polarized excited states makes the loss of optical circular polarization more dependent on the spin flips *via* phonon-assisted scattering processes.

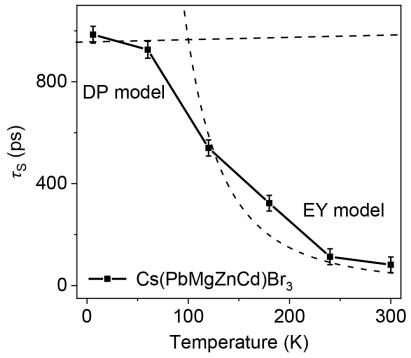

Figure R4. Temperature dependence of τ_S for Cs(PbMgZnCd)Br_3 nanocrystals, extracted by fitting the optical Hanle curves at various temperatures. The black dashed lines represent the temperature dependence according to the EY model and the DP model, respectively.

Accordingly, we have supplemented **Figure R4** as **Figure S28**, and the discussions have also been added in the main text (page 8, 11) as well as Supplementary Information.

5. In another note, Rashba splitting generate a difference in k vector basically changing a direct gap into an indirect gap. In this way, one would expect an elongated charge recombination lifetime and suppressed PL emission. In the experiment, an opposite

trend is observed where high entropy alloy decreases the recombination lifetime with higher PL quantum yield. The authors should probably also explain this point on how the larger Rashba splitting can generate shorter recombination lifetime.

Our Response: We agree with Reviewer #1 that Rashba splitting can introduce a momentum-space offset and an indirect-gap character in the band structure. It typically leads to slow charge recombination and low photoluminescence efficiency. In the high-entropy $Cs(PbMgZnCd)Br_3$ nanocrystals, the size of emissive $[PbBr_6]^{4-}$ domains is below the exciton Bohr radius. Therefore, the quantum confinement effect reduces the band dispersion and relaxes the momentum selection rule, similar to that observed in silicon quantum dots (added as ref. 34, *Nat. Nanotechnol.* **2014**, *9*, 19-32). The structural confinement in high-entropy nanocrystals can be observed from the HRTEM images of high-entropy perovskite nanocrystals with various M/Pb ratios, as shown in **Figure R5**, which explains the blue shift of photoluminescence bands as well as the higher PLQYs. The larger Rashba splitting cannot generate shorter recombination lifetime; instead, it may prolong the recombination lifetime. It is the quantum confinement effect in the high-entropy structures that suppresses the indirect-gap features and facilitates the radiative recombination and improves the photoluminescence efficiency.

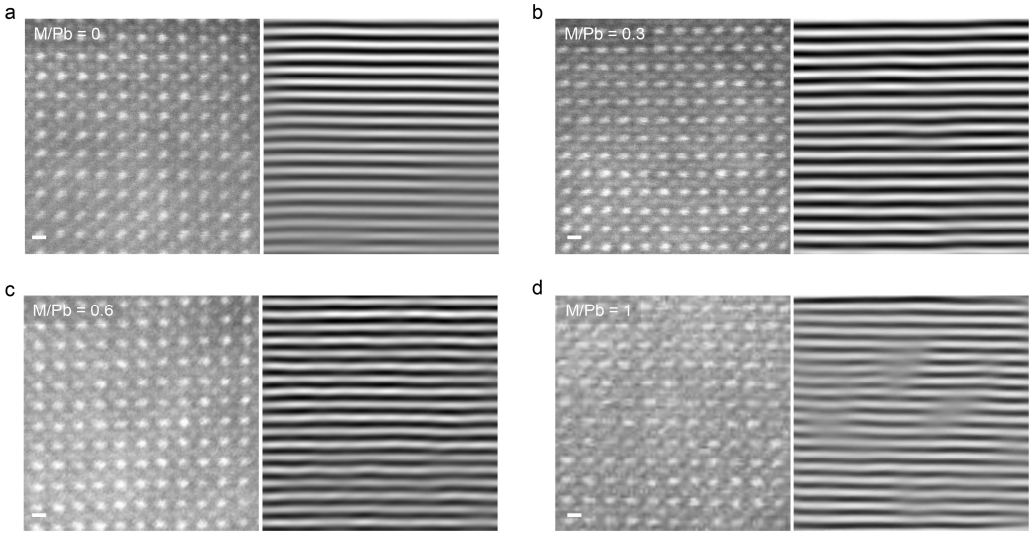

Figure R5. Atomic inverse fast Fourier transform filtered image derived from the HRTEM images

of high-entropy LHPs with various M/Pb ratios.

Accordingly, we have supplemented **Figure R5** as **Figure S7**, and the discussions have also been added in the main text (page 6) as well as Supplementary Information.

6. Amplified spontaneous emission from $CsPbBr_3$ nanocrystals should also be measured. Can the circular polarization of ASE be observed at room temperature for $CsPbBr_3$ nanocrystals?

Our Response: Following Reviewer #1's comments, we have measured ASE from $CsPbBr_3$ nanocrystals, and examined its circular polarization under circularly polarized pump at room temperature, as shown in **Figure R6a**. $CsPbBr_3$ nanocrystals exhibit a clear ASE peak at ~546 nm under a pump fluence of 7.7 μJ cm^{-2}; however, no discernible circular polarization is detected in the ASE emission.

Although the radiative lifetime of $CsPbBr_3$ nanocrystals is significantly shortened under ASE conditions (~5.3 ns, **Figure R6b**), it remains much longer than the spin relaxation time (~4.6 ps). According to the relation $P \sim \frac{1}{1+\tau_R/\tau_S}$, the expected degree of circular polarization of ASE is <0.1%, which is still below the detection limit of our experimental setup. The absence of circularly polarized ASE at room temperature from $CsPbBr_3$ nanocrystals further highlights the unique properties combining photo-physics and spin-physics in the high-entropy perovskite nanocrystals.

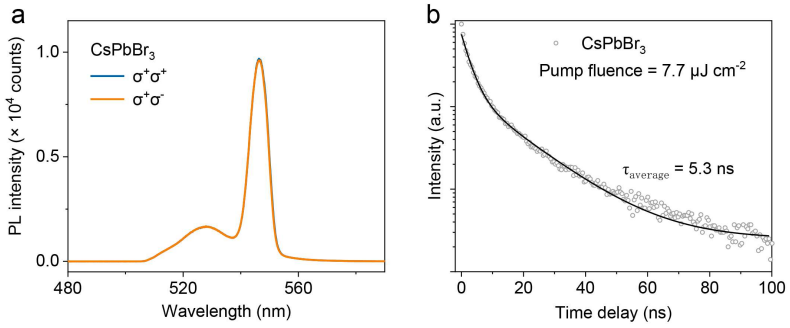

Figure R6. (a) Circularly polarized (σ^+ and σ^-) ASE under σ^+ laser pulses (λ_{ex} = 480 nm) from $CsPbBr_3$ (pump fluence = 7.7 μJ cm^{-2}). (b) The PL decay dynamics of $CsPbBr_3$ nanocrystals under

pump fluences of 7.7 μJ cm^{-2}.

Accordingly, we have supplemented **Figure R6** as **Figure S33**, and the discussions have also been added in the main text (page 11) as well as Supplementary Information.

7. For the results of temperature dependence (for instance, Fig. 5d and 5e), the authors attribute it to the suppression of phonon-assisted thermal perturbations. Is there any contribution from the structural change or phase transition at cryogenic temperatures?

Our Response: Following Reviewer #1's comments, we have performed temperature-dependent XRD measurements of both $CsPbBr_3$ and $Cs(PbMgZnCd)Br_3$ from 300 to 80 K, as shown in **Figure R7**. The results show no obvious changes in diffraction patterns in a wide temperature range, which is consistent with the previous report that phase transitions in $CsPbBr_3$ perovskites occur above room temperature (added as ref. 25, *J. Phys. Soc. Japan* **1974**, *37*, 1393-1398). In addition, the structural change or phase transition may lead to a sudden change of PL intensity/wavelength, or the emergence of a secondary PL band. In the $Cs(PbMgZnCd)Br_3$ nanocrystals, the PL peak gradually redshifts upon cooling (**Figure S9**), which can be attributed to suppressed phonon-assisted processes and bandgap renormalization, as previously reported for lead halide perovskites (added as ref. 39, *J. Phys. Chem. Lett.* **2019**, *10*, 2546-2553).

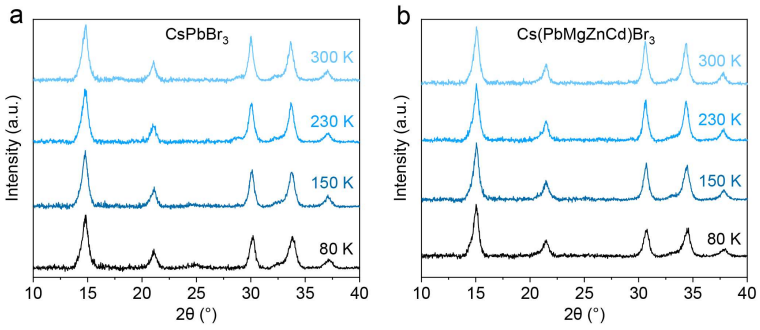

Figure R7. Temperature-dependent XRD patterns of $CsPbBr_3$ and $Cs(PbMgZnCd)Br_3$ nanocrystals recorded under different temperatures (300-80 K).

Accordingly, we have supplemented **Figure R7** as **Figure S2**, and the discussions

have also been added in the main text (page 3) as well as Supplementary Information.

8. Minor issue: it is better to change P_{PL} into P_{ASE} in Fig. 6b and 6c.

Our Response: We have corrected the labels in **Figure 6b** and **6c** to P_{ASE} in the revised manuscript.

9. Another minor issue, the authors should provide photoinduced spectra for left and right circularly polarized pump to show where the kinetics are taken for better comparison.

Our Response: Following Reviewer #1's comments, we have updated the TA spectra in Figure 4b ($CsPbBr_3$) and Figure 4d ($Cs(PbMgZnCd)Br_3$) to show the decay evolution over a wide time range, and added the $\sigma^+\sigma^+$ and $\sigma^+\sigma^-$ TA spectra from 0 to 300 ps, as shown in **Figure R8**.The $\sigma^+\sigma^+$ and $\sigma^+\sigma^-$ TA dynamics (Figure 4c and Figure 4e) were taken from the TA bands located at ~516 nm for $CsPbBr_3$ nanocrystals and at ~507 nm for $Cs(PbMgZnCd)Br_3$ nanocrystals, respectively.

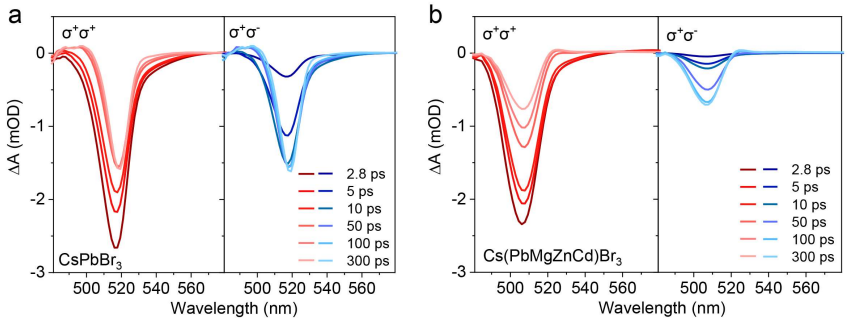

Figure R8. Pump-probe TA spectra in $\sigma^+\sigma^+$ and $\sigma^+\sigma^-$ configurations at different delay times from 0 to 300 ps for (a) $CsPbBr_3$ and (b) $Cs(PbMgZnCd)Br_3$ nanocrystals.

Accordingly, we have supplemented **Figure R8** as **Figure S23**, and the discussions have also been added in the main text (page 8) as well as Supplementary Information.

Reviewer #2

The major advance reported in the paper. This study marks an exciting breakthrough in the field of opto-spintronic halide perovskites by showing, for the first time, that spin-polarized excited states (SPESs) can be observed at room temperature. Until now, such studies were only possible at cryogenic temperatures because of fast spin relaxation and poor photoluminescence efficiency under ambient conditions. The authors overcame this challenge by using high-entropy Cs(PbMgZnCd)Br_3 perovskites, where the presence of multiple metal cations creates strong lattice distortions in the $[PbBr_6]^{4-}$ framework. These distortions enhance Rashba spin–orbit coupling, allowing the excitons to maintain their spin polarization for longer times. As a result, circularly polarized light could be used to probe SPESs even at room temperature. This is a major step forward, as it brings the study of spin phenomena closer to real-world device applications. Beyond the immediate results, the work highlights how high-entropy design can be a powerful approach to tune spin dynamics and structural properties in perovskites, paving the way for the development of next-generation room-temperature opto-spintronic materials.

Our Response: We sincerely appreciate Reviewer #2 for the very positive evaluation as well as the time and efforts in examining our manuscript. Below is our point-by-point response to his/her comments, and corresponding revisions have been made to the main text, figures, as well as Supplementary Information.

Technical suggestion:

1. Frequent references to multiple figures within the same paragraph can disrupt the flow of reading and make it difficult for readers to maintain focus. Reducing such repetition and integrating figure references more strategically would improve clarity and enhance the overall readability of the article.

Our Response: According to Reviewer #2's comments, we have carefully examined

and revised the manuscript to streamline figure references and improve the overall flow of the main text.

2. The study mentions the spatial distribution of Pb, Mg, Zn, and Cd in the nanocrystals but does not provide detailed statistical analysis or quantitative data on the uniformity of doping. Variations in doping levels could impact the reproducibility and performance of the material. Quantitative data obtained by SEM-EDS or TEM-EDS can be included.

Our Response: According to Reviewer #2's comments, we have performed SEM-EDS measurements on 20 parallel samples of $Cs(PbMgZnCd)Br_3$ and provided detailed statistical analysis, as shown in **Figure R9**. It shows that the composition of high-entropy perovskite nanocrystals is highly reproducible, and the distributions on elemental compositions (Pb ~30%, Mg ~20%, Zn ~24%, and Cd ~26%) are very narrow. The thermodynamically favored product is supposed to be governed by the interplay between configurational entropy and the solubility of MBr_2 salts during the ion-exchange process. Meanwhile, the photoluminescence of high-entropy perovskite nanocrystals is also reproducible, as shown in **Figure R10**. The very narrow distribution centered at ~515 nm is related to exciton confinement determined by the distribution of Pb and non-Pb metal ions, further verifies the high reproducibility of as-prepared high-entropy nanocrystals.

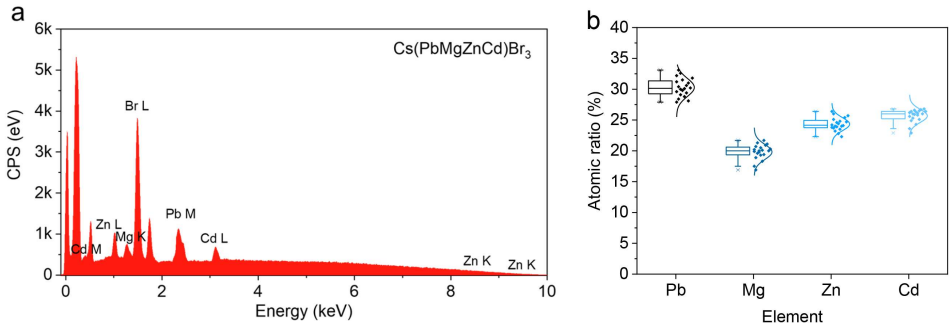

Figure R9. (a) Representative SEM–EDS spectrum of $Cs(PbMgZnCd)Br_3$ nanocrystals, showing the characteristic X-ray peaks of Pb, Mg, Zn, Cd, and Br. (b) distributions of Pb, Mg, Zn, and Cd atomic ratios obtained from SEM–EDS measurements.

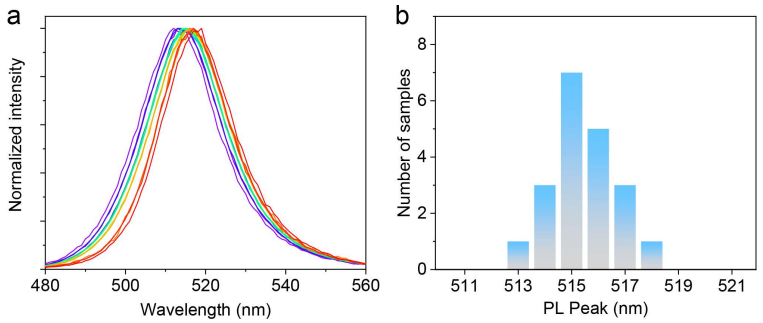

Figure R10. Statistical analysis of 20 parallel samples of Cs(PbMgZnCd)Br_3: (a) PL spectra; (b) the distribution of PL peak wavelengths.

Accordingly, we have supplemented **Figure R9** and **Figure R10** as **Figure S4** and **Figure S10**, respectively. The discussions have also been added in the main text (page 4, 6) as well as Supplementary Information.

3. Providing a detailed deeper insight into the mechanisms that prevent non-radiative losses responsible for a high PLQY (~98.5%) for Cs(PbMgZnCd)Br_3 would be beneficial.

Our Response: In the high-entropy perovskites, Mg, Zn, and Cd (denoted as M) are intentionally selected as non-Pb constituents in the high-entropy perovskite owing to their smaller ionic radii compared to Pb^{2+}. The shortened M-Br bonds result in the compressed $[MBr_6]^{4-}$ octahedra, which not only allow for strong lattice distortion but also drive the electronic states associated with the $[MBr_6]^{4-}$ octahedra deep into the valence/conduction bands. Consequently, the non-Pb units are not involved in the band-edge emission, and the excited states remain energetically and spatially confined within the $[PbBr_6]^{4-}$ domains. In the high-entropy Cs(PbMgZnCd)Br_3 nanocrystals, the size of emissive $[PbBr_6]^{4-}$ domains is below the exciton Bohr radius. Therefore, the quantum confinement effect reduces the band dispersion and relaxes the momentum selection rule, similar to that observed in silicon quantum dots (added as ref. 34, *Nat. Nanotechnol.* **2014**, 9, 19-32). The structural confinement in high-entropy nanocrystals explains the blue shift of photoluminescence bands as well as the faster photoluminescence dynamics in high-entropy perovskite nanocrystals with various

M/Pb ratios, as shown in **Figure R11**. The spatially confined excited state reduces the probability of interacting with non-radiative recombination centers due to the suppressed migration across the lattice, which is supported by the excitation power dependence of photoluminescence intensities (**Figure 3c**). $CsPbBr_3$ exhibits a pronounced sub-linear intensity-power dependence (k = 0.76), whereas $Cs(PbMgZnCd)Br_3$ displays an almost ideal linear relationship (k = 1.0). The quantum confinement of excitons within the isolated $[PbBr_6]^{4-}$ domains in high-entropy perovskites facilitates the radiative recombination and prevents non-radiative losses, leading to the blue-shifted photoluminescence with a high PLQY.

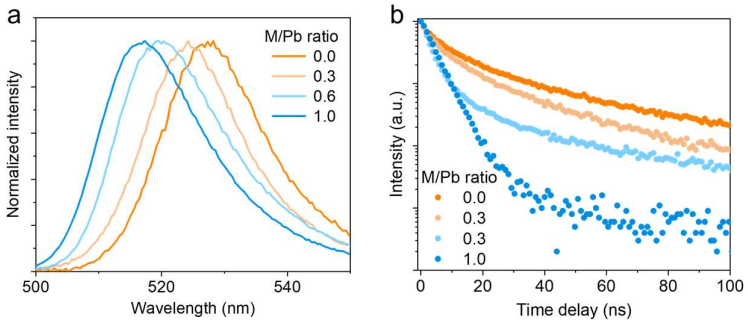

Figure R11. PL spectra (a) and PL decay dynamics (b) measured for the high-entropy LHPs with various M/Pb ratios.

Accordingly, we have supplemented **Figure R11** as **Figure S8**, and the discussions have also been added in the main text (page 5, 6) as well as Supplementary Information.

4. In Figure 5, ensuring that the caption and the figure appear on the same page would improve visual appearance.

Our Response: We have adjusted the manuscript layout to ensure that figures and their captions appear on the same page to improve visual appearance presentation.

5. The overall text alignment and formatting could be enhanced to improve readability and coherence. It is recommended to ensure consistent font size, margins, and spacing throughout the manuscript.

Our Response: We have checked the font size, margins, and spacing throughout the manuscript to meet the criteria of text alignment and formatting for a high-profile paper.

6. Including a discussion on specific future research directions would help contextualize the broader impact of the study and guide subsequent investigations in the field.

Our Response: We appreciate Reviewer #2 for his/her insightful comments**.** In the revised manuscript, we have included a few sentences in the Discussion section (page 13) to highlight future research directions that could be inspired by our results.

"The compositional and structural engineering of high-entropy perovskites may further overcome current limitations in key spin-related parameters and help clarify the spin relaxation mechanisms in LHPs. This would benefit the construction of room-temperature spintronic devices for both optical and electronic categories based on LHPs. In addition, incorporating the high-entropy nanocrystals into microcavity or waveguide platforms may be useful for the manipulation of spin-polarized states on integrated photonic chips towards quantum information processing."

Reviewer #3

This work reports a compelling study of spin-dependent excitonic properties in a high-entropy material, Cs(PbMgZnCd)Br_3 nanocrystals. An exceedingly long spin relaxation time up to ~60ps is realized, accompanied by a short radiative recombination (~3.4ns), leading to possible spin control of spin-polarized excitonic states at room temperature. This study is centered on an equation describing the correlation between the circular polarization of emission and a ratio of spin relaxation time to radiative recombination time, as shown on page 9. To increase the spin relaxation time while reducing the radiative time, this work aimed to tailor the spin-dependent properties of nanocrystals by inducing substitutional elements into $CsPbBr_3$ nanocrystals. The high-entropy structure of Cs(PbMgZnCd)Br_3 induces a large Rashba splitting state that can significantly increase the spin relaxation time, while the excitonic confinement reduces the radiative time. The large circular polarization is demonstrated by circularly polarized TA and optical Hanle measurements. Another compelling result in this work is to utilize the short radiative time during the ASE process, resulting in a large circular polarized ASE up to 26% at room temperature. Remarkably, this work also reported the first optical Hanle effect of circular polarized ASE, fully demonstrating the optical access of spin-polarized excitonic state under a magnetic field. This is a complete work highlighting the great potential of circularly polarized PL/ASE for spin control. The manuscript is well-organized, and the data quality is marvelous. Thus, I would recommend the publication of this work in Nature Communications after the following comments are fully addressed.

Our Response: We sincerely appreciate Reviewer #3 for the very positive and his/her time and efforts in examining our work. A point-by-point response to Reviewer #3's comments is provided as below, and the revised parts in the manuscript as well as the Supporting Information have been highlighted accordingly.

1. What's the key rationale to choose a composition including Mg, Zn, and Cr? I understand the current composition can induce excitonic confinement. However, if a

large Rashba splitting requires strong SOC, should the Pb be replaced by higher SOC elements instead of lower ones?

Our Response: Our motivation is that the replacement of Pb with much smaller B-site cations can introduce a strong lattice distortion in the $CsPbBr_3$ lattice. However, the Goldschmidt tolerance factor has to be taken into account for single-metal doping in perovskite structures (added as ref. 28, *Sci. Adv.* **2019**, *5*, eaav0693). The high-entropy perovskites can overcome the above structural limitations and enable high-level multi-metal doping (e.g., Mg, Zn, Cd) in the rigid $CsPbBr_3$ lattice (ref. 24, *J. Am. Chem. Soc.* **2022**, *144*, 5864-5870).

More importantly, the sizes of M ions are all smaller than Pb^{2+}, and the shorter M-Br bonds strengthen the orbital hybridization, pushing the $[MBr_6]^{4-}$-related states deep into the valence/conduction bands. In this case, the CBM and VBM are still composed of Pb and Br orbitals, so the SOC strength therein should remain almost the same for high-entropy $Cs(PbMgZnCd)Br_3$. The $[PbBr_6]^{4-}$ octahedra, where the excited states are spatially confined, are the only emission centers, while the $[MBr_6]^{4-}$ octahedra are not expected to contribute to band-edge emission. The strong lattice distortion enhances the inversion-symmetry breaking, thereby the Rashba splitting shows a larger momentum offset in $Cs(PbMgZnCd)Br_3$ (k_R = 0.305 $Å^{-1}$) compared with $CsPbBr_3$ (k_R = 0.053 $Å^{-1}$).

We agree that replacing Pb with heavier elements is an alternative (and possibly a better) way to enhance the Rashba effect in lead halide perovskites. Unfortunately, it remains challenging in the design and synthesis of these types of high-entropy materials, which definitely merits our efforts in future studies.

Accordingly, the above discussions and related references have been added in the main text (page 4) as well as Supplementary Information.

2. The claimed large Rashba spin splitting needs to be validated. What's the value of the Rashba parameter compared to that in the conventional $CsPbBr_3$ NCs? On page 8,

the calculations show the energy splitting and momentum shift in two compounds. From these values, the calculated Rashba parameter in $CsPbBr_3$ (1.28 eVA) is larger than that in the $Cs(PbMgZnCd)Br_3$ (0.89 eVA). This contradicts the main statement about the increase in spin relaxation time due to the formation of a larger Rashba state. In addition, do authors conduct any CPGE measurement to validate the spin-momentum correlation? Only the DFT calculation does not adequately prove the presence of the Rashba splitting.

Our Response: In the systems with Rashba effect, the band splitting is characterized by both an energy scale (E_R) and a momentum offset (k_R, i.e., the k-space splitting), which together determine the spin texture of the band-edge states. In this work, both E_R and k_R are enhanced in high-entropy $Cs(PbMgZnCd)Br_3$ compared with conventional $CsPbBr_3$. The calculated E_R and k_R values for $CsPbBr_3$ are consistent with those reported previously (ref. 45, *ACS Nano* **2025**, *19*, 31331-31339). The limited increase in E_R arises from the fact that the effective SOC in $Cs(PbMgZnCd)Br_3$ is still primarily contributed by the $[PbBr_6]^{4-}$ octahedra, and its overall strength therefore remains largely unchanged. In contrast, the pronounced lattice distortions in $Cs(PbMgZnCd)Br_3$ break the inversion symmetry effectively, and the k-space splitting k_R increases by one order of magnitude (from 0.053 to 0.305 $Å^{-1}$). We realize that spin relaxation in $CsPbBr_3$ and other types of lead-halide perovskites is typically controlled by the phonon-assisted spin relaxation pathways, which is mainly determined by k_R rather than E_R in the Rashba sin splitting (added as ref. 46, *J. Am. Chem. Soc.* **2024**, *146*, 12225-12232; added as ref. 47, *J. Phys. Chem. Lett.* **2025**, *16*, 5681-5686).

Following Reviewer #3's comments, we have performed circular photogalvanic effect (CPGE) measurements on both $CsPbBr_3$ and $Cs(PbMgZnCd)Br_3$, as shown in **Figure R12**. The nanocrystals were mixed with poly(vinylcarbazole) (PVK) in the precursor solution, which was spin coated on interdigitated Au electrodes prepatterned on the substrate. Under the σ^+/σ^- light illumination by manually rotating the quarter-wave plate, the change of photocurrent under applied biases were observed for both

$CsPbBr_3$ (ΔI_{PC}~0.002 μA) and $Cs(PbMgZnCd)Br_3$ (ΔI_{PC}~0.006 μA). The results prove the spin-momentum correlation in Rashba splitting, caused by the strong SOC and inversion symmetry breaking in $CsPbBr_3$ and $Cs(PbMgZnCd)Br_3$ nanocrystals (added as ref. 44, *Nat. Commun.* **2020**, *11*, 323).

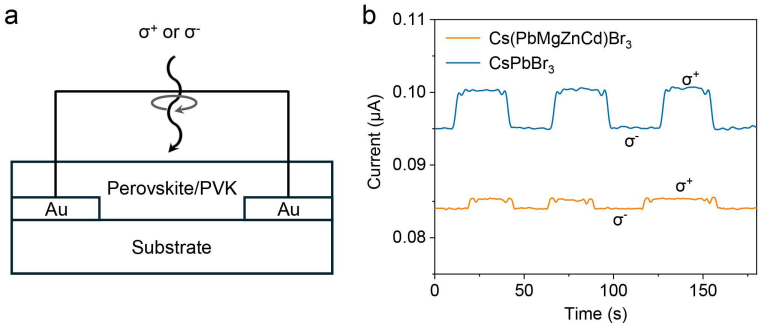

Figure R12. (a) Schematic of device geometry for circular photogalvanic effect (CPGE) measurements. (b) Photocurrent of $CsPbBr_3$ and $Cs(PbMgZnCd)Br_3$ under alternating σ^+/σ^- light illumination.

Accordingly, we have supplemented **Figure R12** as **Figure S20**, and the related discussions have been added in the main text (page 8) and Supplementary Information.

3. Could authors provide a table to compare the obtained tau_s in other compounds from literature reports? Is this value of 34ps adequately long?

Our Response: Following Reviewer #3's comments, we have supplemented **Table R1** to compare the reported spin lifetimes (τ_S) of perovskites (added as ref. 52, *J. Phys. Chem. Lett.* **2025**, *16*, 5109-5120). Most τ_S values in previously reported lead halide perovskites typically fall below ~10 ps at room temperature. Specifically, τ_S for $CsPbBr_3$ nanocrystals is measured to be ~4.6 ps in this work, which agrees well with previous studies. In comparison, the high-entropy $Cs(PbMgZnCd)Br_3$ nanocrystals show a much longer τ_S of ~59.8 ps at room temperature, which is remarkably long compared with lead and even non-lead perovskite materials.

Accordingly, we have supplemented **Table R1** as **Table S3**, and the discussions

have also been added in the main text (page 9) as well as Supplementary Information.

Table R1. Summary of spin lifetime measured in perovskites.

Perovskites	Morphology	Spin lifetime	Refer.
$Cs(PbMgZnCd)Br_3$	NCs	59.8 ps	**This work**
$CsPbBr_3$	NCs	4.6 ps	**This work**
	NCs	4.4 ps	*ACS Energy Lett.* **2022**, *7*, 4325–4332
	QDs	1.2 ps	*Nat. Nanotechnol.* **2023**, *18*, 124–130
	Film	3.8 ps	*J. Phys. Chem. Lett.* **2020**, *11*, 1502–1507
	Bulk	3.2 ps	*Sci. Adv.* **2020**, *6*, eabb7132
$MAPbBr_3$	SC	3.1 ps	*J. Phys. Chem. Lett.* **2018**, *9*, 2595–2603
	Film	4.3 ps	*J. Phys. Chem. Lett.* **2020**, *11*, 1502–1507
	Film	3.5 ps	*J. Phys. Chem. Lett.* **2018**, *9*, 2595–2603
$CsPbI_3$	NCs	3.9 ps	*Science* **2021**, *371*, 1129-1133
	QDs	3.2 ps	*ACS Energy Lett.* **2020**, *5*, 1701–1708
	2D NPs	0.9 ps	*Sci. Adv.* **2020**, *6*, eabb7132
	Film	3.2 ps	*Sci. Adv.* **2020**, *6*, eabb7132
	Film	2.2 ps	*J. Phys. Chem. Lett.* **2020**, *11*, 1502–1507
$MAPbI_3$	SC	1.5 ps	*ACS Energy Lett.* **2018**, *3*, 2273–2279
	Film	1.37 ps	*J. Phys. Chem. Lett.* **2018**, *9*, 2595–2603
	Film	2.2 ps	*J. Phys. Chem. Lett.* **2020**, *11*, 1502–1507
	Film	4 ps	*Nano Lett.* **2015**, *15*, 1553–1558
$CsSnBr_3$	NCs	18.0 ps	*ACS Energy Lett.* **2021**, *6*, 1670–1676
$MAPbIBr_2$	Film	3.3 ps	*J. Phys. Chem. Lett.* **2020**, *11*, 1502–1507
$MAPbI_2Br$	Film	2.3 ps	*J. Phys. Chem. Lett.* **2020**, *11*, 1502–1507
$CsPb(Br_{0.1}I_{0.9})_3$	NCs	14.2 ps	*Science* **2021**, *371*, 1129-1133
$BA_2FAPb_2I_7$	Film	3.2 ps	*Nano Lett.* **2020**, *20*, 5678–5685
$(EIA)_2(MA)_{n-1}PbnI_{3n+1}$	2D film	1.6 ps (n=1) 15.2 ps (n=2)	*Angew. Chem. Int. Ed.* **2023**, *62*, e202304486
$PEA_2PbI_4{\cdot}(MAPbI_3)_{n-1}$	SC	0.3 ps (n=1) 3.0 ps (n=2) 3.2 ps (n=3) 7.0 ps (n=4)	*ACS Energy Lett.* **2018**, *3*, 2273–2279

4. It is stated that the D'yakonov-Perel mechanism is responsible for the larger spin relaxation time in the presence of Rashba splitting. The Rashba splitting does not

guarantee the DP model. Have the authors conducted a plot of tau_s as a function of tau_p to validate the DP mechanism?

Our Response: We appreciate Reviewer #3 for the insightful comments on spin relaxation mechanisms, and we agree that the Rashba splitting does not guarantee the Dyakonov-Perel (DP) mechanism. The Rashba splitting is characterized by both an energy scale (E_R) and a momentum offset (k_R, i.e., the k-space splitting), which together determine the spin texture of the band-edge states. The spin relaxation is typically controlled by the phonon-assisted spin relaxation pathways, which have been studied in $CsPbBr_3$ and other lead-halide perovskites (added as ref. 46, *J. Am. Chem. Soc.* **2024**, *146*, 12225-12232; added as ref. 47, *J. Phys. Chem. Lett.* **2025**, *16*, 5681-5686). DP type spin relaxation (spin dephasing) is caused by spin precession in a *k*-dependent spin-orbit field continuously randomized by phonon-induced momentum scattering, while Elliott-Yafet (EY) type spin relaxation (spin flips) occurs due to SOC-induced spin mixing of the electronic states during phonon scattering. In the high-entropy perovskites, the larger k-space splitting associated with the enhanced Rashba effect is consistent with the observed slower spin relaxation. The momentum mismatch between spin-polarized excited states makes the loss of optical circular polarization more dependent on the spin flips via phonon-assisted scattering processes.

The relationship between spin relaxation time τ_S and the momentum relaxation time τ_P can provide direct validation of the underlying spin relaxation mechanisms. Unfortunately, the perovskite nanocrystals are not suitable for long-range transport (or THz conductivity) measurements, and we are not able to measure τ_P using our facilities. Instead, the temperature dependence of τ_S was extracted from the optical Hanle effect measured at various temperatures to study the spin relaxation mechanisms (added as ref. 52, *J. Phys. Chem. Lett.* **2025**, *16*, 5109-5120). Notably, the experimental τ_S values as a function of T cannot be described by either the DP model or the EY model over the entire temperature range, as shown in **Figure R13**. The DP model seems to be more pronounced at low temperatures while the EY model is likely dominant at high

temperatures, possibly because the SOC-induced spin flips occur more frequently via the enhanced phonon scattering. Therefore, it is probably a combination of DP and EY mechanisms, and the recombination/trapping and inhomogeneous broadening may also contribute to the spin relaxation especially at room temperature.

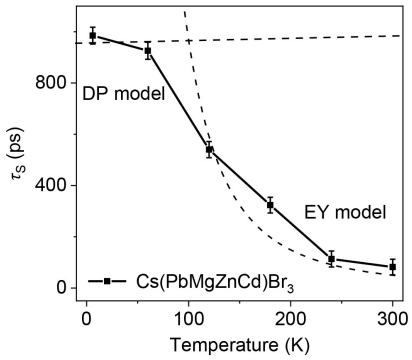

Figure R13. Temperature dependence of τ_S for Cs(PbMgZnCd)Br_3 nanocrystals, extracted by fitting the optical Hanle curves at various temperatures. The black dashed lines represent the temperature dependence according to the EY model and the DP model, respectively.

Accordingly, we have supplemented **Figure R13** as **Figure S28**, and the related discussions have been added in the main text (page 11) and Supplementary Information.

Minor issues in SI:

5. What are the red and dark plots in Fig. S7? Please update the caption accordingly.

Our Response: The integrating-sphere setup was used for the PLQY measurements, in which system dark and stray light signals were recorded for background subtraction. The red and black plots in **Figure S7** are the raw emission spectrum of the sample and the background spectrum recorded under the same conditions. The caption of **Figure S7** has been updated as **Figure S13** accordingly in the revised Supporting Information.

6. Is there any phase transition that can cause a blueshift of PL as temperature increases, as shown in Fig. S9?

Our Response: We have performed temperature-dependent XRD measurements of

both $CsPbBr_3$ and $Cs(PbMgZnCd)Br_3$ from 300 to 80 K, as shown in **Figure R14**. The results show no obvious changes in diffraction patterns, which is consistent with the previous report that phase transitions in $CsPbBr_3$ occur above room temperature (added as ref. 25, *J. Phys. Soc. Japan* **1974**, *37*, 1393-1398). In addition, the structural change or phase transition may lead to a sudden change of photoluminescence intensity/wavelength, or the emergence of a secondary photoluminescence band. In the $Cs(PbMgZnCd)Br_3$ nanocrystals, the photoluminescence peak gradually redshifts upon cooling (**Figure S9**), which can be attributed to suppressed phonon-assisted processes and bandgap renormalization, as previously reported for lead halide perovskites (added as ref. 39, *J. Phys. Chem. Lett.* **2019**, *10*, 2546–2553).

Accordingly, we have supplemented **Figure R14** as **Figure S2**, and the discussions have also been added in the main text (page 3) as well as Supplementary Information.

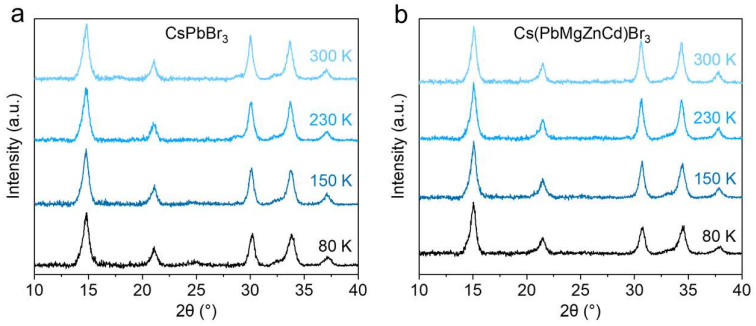

Figure R14. Temperature-dependent XRD patterns of $CsPbBr_3$ and $Cs(PbMgZnCd)Br_3$ nanocrystals recorded under different temperatures (300 - 80 K).

7. Fig. S8 and Fig. S13 are band structures for the same $CsPbBr_3$ at different k vectors. Is there no Rashba spin splitting between gamma-Z, gamma-Y, etc?

Our Response: We appreciate Reviewer #3 for the careful reading, and we provide a detailed description of the band structure calculations as follows.

The band structure in **Figure S8** is obtained by the Tran-Blaha modified Becke-Johnson (TB-mBJ) method without considering the contribution of SOC. The

calculations were carried out to reveal the role of non-Pb metals in the band structure, where the electronic states associated with the $[MBr_6]^{4-}$ octahedra locate deep into the valence/conduction bands (**Figure 3d**). It helps to prove that the $[PbBr_6]^{4-}$ octahedra are the only emission centers in the high-entropy perovskites. Therefore, no Rashba splitting appears because no SOC contribution is involved.

In comparison, the results in **Figure S13** are calculated by the Heyd–Scuseria–Ernzerhof (HSE06) hybrid functional method and SOC is taken into account within the first-principles framework as implemented in the VASP code. Because the $CsPbBr_3$ nanocrystals in this work preferentially expose (101)-oriented crystal facets, we used a (101)-oriented monolayer of corner-sharing $[PbBr_6]^{4-}$ octahedra as the model for the band structure calculations, as shown in **Figure R15**. Therefore, the inversion-symmetry breaking is perpendicular to the interface, i.e., along the out-of-plane direction, and the Rashba splitting is expected to be pronounced within the plane of the (101)-oriented monolayer, i.e., the Γ–R and Γ–T paths in the orthorhombic Brillouin zone. When SOC is included and inversion symmetry is broken, Rashba splitting becomes clearly visible along these directions.

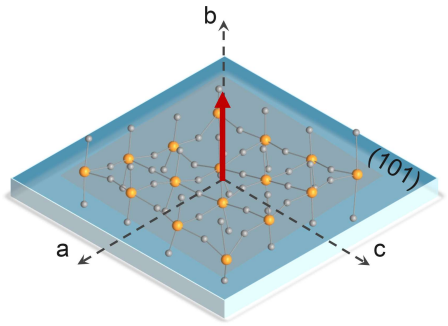

Figure R15. Schematic of a (101)-oriented monolayer of $[PbBr_6]^{4-}$ octahedra in $CsPbBr_3$. The red arrow indicates the direction of inversion-symmetry-breaking.

Accordingly, we have supplemented **Figure R15** as **Figure S19**, and the related descriptions/discussions for band structure calculations have been added in the main text (page 8) as well as Supplementary Information.

8. Fig. S26 indicates this is 'laser emission'. Would this be ASE emission only?

Our Response: We have corrected the caption of **Fig. 26** to ASE emission accordingly.

Response to Reviewers' Comments (NCOMMS-25-80800A)

Reviewer #1

The author have addressed most of my concerns. I just have one comment related to my previous comment 5 that Rashba splitting should reduce PL emission instead of enhancing it. The authors explained with quantum confinement effect and exciton Bohr radius. This may still not be the cause of enhanced PL emission as these two effects does not directly influence k-vector which governs the PL emission efficiency. I think maybe this article could help the authors to explain the Rashba trend that the k-vector tuning could help PL emission. ACS Nano 2025, 19, 35, 31331-31339. I am wondering if the quantum dots the authors synthesized could experience the same type of k-vector aligning. Apart from this point, I think this paper is in good shape to be published.

Our Response: We sincerely appreciate Reviewer #1 for his/her insightful comments. We agree that the k-vector difference between the valence band (VB) and the conduction band (CB) governs the PL emission efficiency, and the spin-orbit coupling (SOC) combined with inversion symmetry breaking can induce spin splitting in both the VB and CB. In the literature (ref. 34, B. A. Ali & C. B. Musgrave, *ACS Nano* **2025**, *19*, 31331-31339.), the enhanced Rashba splitting may align the VB maximum (VBM) and CB minimum (CBM) in k-space and brighten the excitonic ground state. In our high-entropy nanocrystals, the enhanced PL emission may also be related to the k-vector alignment of the VBM and CBM due to the Rashba-type SOC. It is consistent with the experimental observation that the radiative recombination rate gradually increases when the lattice becomes more distorted in high-entropy Cs(PbMgZnCd)Br_3 (Figure S8). Meanwhile, the quantum confinement effect can further reduce the band dispersion and relax the momentum selection rule, which is validated by the blue-shift of the PL band from high-entropy nanocrystals (Figure 3b).

Accordingly, we have added ref. 34 and the above discussion in the revised main text (page 6).

Reviewer #3

The authors have carefully addressed most of the comments; however, I remain unsatisfied with one specific response.

In my previous comment (#2), I suggested conducting CPGE measurements to validate the presence of the Rashba splitting in Cs(PbMgZnCd)Br$_3$, as this is the only viable characterization approach to directly probe the Rashba state. However, the device geometry utilized by the authors (Fig. R12) represents a typical circularly polarized photodetector configuration rather than a proper CPGE setup.

For valid CPGE measurements, the detected photocurrent must be transverse to the plane of the incident laser due to the well-established spin-momentum locking at the Rashba state. Furthermore, the authors need to perform laser incidence angular-dependent measurements of the CPGE photocurrent. Specifically, they need to demonstrate that the sign of the photocurrent inverts when the angle of laser incidence is reversed. Without this angular dependence and the correct transverse geometry, the results cannot be definitively attributed to the Rashba effect.

Our Response: We sincerely appreciate Reviewer #3 for his/her insightful comments. Also, we apologize that we have very limited expertise in the CPGE measurements. According to Reviewer #3's comments as well as the detailed description in previous literature (ref. 44, X. Liu, et al., *Nat. Commun.* **2020**, *11*, 323.), we have re-performed the CPGE experiment, as shown in **Figure R1**. As we did not have the capability to finely tune the laser incident angle θ, we fixed it at the maximum value (approximately +45° and -45°) limited by the size of the optical window. In addition, the photocurrent is transverse to the plane of the incident laser to ensure the spin-momentum locking in the Rashba state. Under σ^+/σ^- light illumination by manually rotating the quarter-wave plate, the change of photocurrent is observed for both $CsPbBr_3$ and $Cs(PbMgZnCd)Br_3$ devices, and the sign of the photocurrent change inverts when the angle of the laser incidence is reversed. The average CPGE values for $CsPbBr_3$ and $Cs(PbMgZnCd)Br_3$

are ~2.8% and ~1.1%, respectively, which provide direct experimental evidence to validate the presence of the Rashba effect in high-entropy nanocrystals.

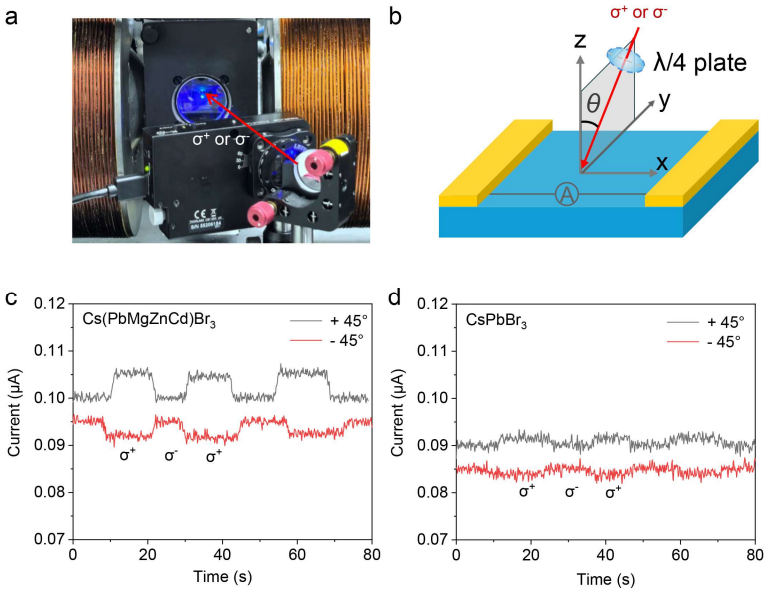

Figure R1. (a) Experimental setup and (b) schematic illustration of the device geometry for circular photogalvanic effect (CPGE) measurements. Photocurrent measured from (c) $Cs(PbMgZnCd)Br_3$ and (d) $CsPbBr_3$ devices under σ^+/σ^- light illumination at incident angles of +45° and -45°.

Accordingly, we have updated the illustration of device geometry and the results of CPGE experiments in Figure S20, as well as the related description/discussion in the main text (page 7) and the Supplementary Information.

Response to Reviewers' Comments (NCOMMS-25-80800B)

Reviewer #1

The authors have addressed all my comments. The paper can now be accepted.

Our Response: We are grateful that the manuscript is recommended for acceptance and appreciate Reviewer #1 for his/her efforts in helping us improve our work.

Reviewer #3

The authors have addressed my concern about CPGE measurements. Now, I recommend publishing this work as is.

Our Response: We are grateful that the manuscript is recommended for publication and appreciate Reviewer #3 for his/her efforts in helping us improve our work.

Reviewer #4

This work reports the synthesis and optical characterization of high-entropy perovskite colloidal nanocrystals, Cs(PbMgZnCd)Br$_3$, in which partial substitution of Pb^{2+} with a mixture of Mg^{2+}, Zn^{2+}, and Cd^{2+} creates isolated and distorted $[PbBr_6]^{4-}$ luminescent domains. The authors demonstrate that this structural engineering simultaneously shortens the radiative lifetime (τ_R ~ 3.4 ns) via quantum confinement and prolongs the spin relaxation time (τ_s ~ 59.8 ps) via enhanced Rashba spin splitting, enabling optical write-in and read-out of spin-polarized excited states at room temperature with a circular polarization up to 25.8% in amplified spontaneous emission.

Our Response: We appreciate Reviewer #4 for his/her efforts in examining our work, as well as the insightful comments for us to further improve the manuscript. A "point-by-point" response is provided as below, and the revised parts are also highlighted in the main text as well as Supplementary Information.

We would like to point out that research on high-entropy perovskites, particularly their photo-physical and spin-physical properties, is still at its very early stage (refer to the pioneering work in Folgueras, et al., *Nature* **2023**, *621*, 282-288). Here our experimental study reveals that high-entropy engineering can prolong spin relaxation time of perovskite materials, and we achieve optical write-in and read-out of spin-polarized excited states at room temperature. These main conclusions have been highly recognized by Reviewers #1 to #3, and all their previous concerns have been fully addressed. Following Reviewer #4's suggestions, we have tried our best to supplement additional experimental results and to clarify underlying mechanisms related to these observations. Nevertheless, we have to be honest that some aspects of quantitative analysis and microscopic mechanisms still merit further efforts in future studies, limited by experimental capabilities and theoretical understanding at current stage. Therefore, in the 3rd revised version we have either provided direct experimental evidence to fully support qualitative conclusions, or offered plausible interpretations for detailed analysis and further discussion. Once again, we sincerely appreciate Reviewer #4 for his/her valuable comments, and we hope that our efforts, explanations and revisions make sense to him/her.

1. The authors propose that high-entropy doping spatially partitions the $[PbBr_6]^{4-}$ framework into isolated domains smaller than the exciton Bohr radius, thereby inducing quantum confinement. However, direct and quantitative evidence regarding the actual size, size distribution, and the degree of electronic coupling between these domains is lacking. The current evidence primarily relies on HAADF-STEM contrast analysis and the observation of a PL blue-shift, which are indirect indicators. It is recommended that the authors supplement the study with pair distribution functon (PDF) analysis or small-angle X-ray scattering (SAXS) to provide a more quantitative description of the spatial extent and isolation of the $[PbBr_6]^{4-}$ domains. If such data are unavailable, the speculative nature and associated uncertainties of this structural model should be explicitly addressed in the discussion.

Our Response: We have carried out SAXS measurements on both $CsPbBr_3$ and $Cs(PbMgZnCd)Br_3$ nanocrystal films, as shown in **Figure R1**. The scattering feature at $q \sim 0.165$ Å^{-1} indicates that ordered structures are preserved upon high-entropy alloying. Broad features in the $q = 0.025$-0.100 Å^{-1} region are supposed to be related to the size of nanocrystals or internal domains; however, no clear quantitative difference can be resolved within the current SAXS resolution. This is because the size and spatial distribution of $[PbBr_6]^{4-}$ domains are highly random, and the SAXS signal may also be affected by disordered nanocrystal packing in the film. Unfortunately, we do not have experience with PDF analysis, and currently are not able to get synchrotron beamtime. Qualitatively, HAADF-STEM can directly reveal the existence of small $[PbBr_6]^{4-}$ domains accompanied by structural distortion in high-entropy materials (refer to examples in Ding, et al., *Nature* **2019**, *574*, 223-227; Su, et al., *Nat. Commun.* **2022**, *13*, 2358). The PL blue-shift further verifies that at least a large portion of these domains are below the exciton Bohr radius of $CsPbBr_3$ (~5 nm).

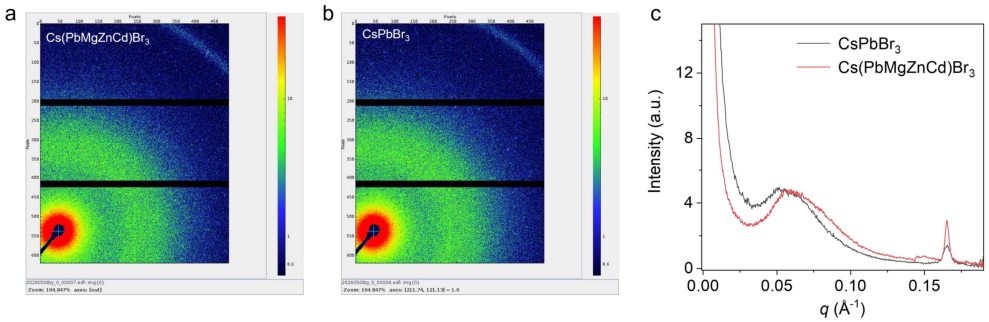

Figure R1. Two-dimensional SAXS patterns of (a) $Cs(PbMgZnCd)Br_3$ and (b) $CsPbBr_3$ nanocrystal films. (c) Corresponding azimuthally integrated one-dimensional SAXS profiles.

Accordingly, we have added **Figure R1** as Figure S6 in the revised version. We have also clarified that the size and spatial distribution of $[PbBr_6]^{4-}$ domains are highly random in high-entropy structure.

2. The authors note that the temperature dependence of the spin relaxation time cannot be adequately fitted by a single D'yakonov-Perel (DP) or Elliott-Yafet (EY) mechanism across the entire temperature range and suggest a combination of both. However, a

detailed analysis of the underlying physical origins for this behavior is missing, and potential contributing factors such as exciton localization, surface states, or defect-assisted scattering are not discussed. Furthermore, details of the fitting attempts shown in Figure S28 are insufficient, making it difficult for the reader to assess the extent of deviation from each model. The authors should provide a more comprehensive analysis, at minimum identifying the dominant mechanism in the low- and high-temperature regimes and discussing how the specific lattice distortions in the high-entropy structure modify the conventional theoretical picture of spin relaxation.

Our Response: The coexistence of DP and EY spin relaxation mechanisms has been previously reported in $CsPbBr_3$ and other Pb-based perovskite materials (Xu, et al., *Nat. Commun.* **2024**, *15*, 188; Tao, et al., *Sci. Adv.* **2020**, *6*, eabb7132). Meanwhile, spin relaxation in perovskite nanocrystals becomes extremely complicated when involving exciton localization, surface states, defect-assisted scattering, and phonon scattering. We would like to clarify that the dashed lines in Figure S28 are guide-for-eye lines rather than fitting attempts. The available experimental data does not allow for detailed analysis to quantitively distinguish spin relaxation mechanisms and influence factors. Qualitatively, EY mechanism should be dominated at room temperature (spin relaxation time is significantly prolonged when it starts cooling down), while DP mechanism is more pronounced at liquid helium temperature (nearly independent on temperature in this range) (refer to Hang, et al., *J. Phys. Chem. Lett.* **2025**, *16*, 5109-5120). It should be also mentioned that spin relaxation in $Cs(PbMgZnCd)Br_3$ and $CsPbBr_3$ follow the same mechanisms, and their temperature-dependent trends of spin relaxation time remain almost unchanged. It is reasonable as high-entropy $Cs(PbMgZnCd)Br_3$ can be considered as nanoscale $CsPbBr_3$ embedded in a wide-gap $Cs(MgZnCd)Br_3$ matrix that is not involved in optical transition or spin relaxation. The lattice distortions in the high-entropy structure do not modify the conventional theoretical picture of spin relaxation; instead, the inversion-symmetry breaking enhances k-space Rashba splitting to slow down spin relaxation despite detailed mechanisms, as suggested by previous reviewers.

Accordingly, we have eliminated Figure S28 to avoid any possible misleading to Reviewer #4 as well as the readers. We have also clarified that spin relaxation remains in the same manner for Cs(PbMgZnCd)Br_3 and $CsPbBr_3$, and EY and DP mechanisms dominate at room temperature and liquid helium temperature, respectively.

3. The fitting of the optical Hanle effect relies on the effective Landé g-factor and the effective lifetime T. While the authors assert that $T \approx \tau_S$ *(based on* $\tau_S \ll \tau_R$*), the explicit g-factor value used in the fitting is not provided, nor is it independently verified. For a high-entropy perovskite with strong spin-orbit coupling, the g-factor may differ from that of pristine* $CsPbBr_3$ *and could exhibit anisotropy. To ensure the reliability of the extracted* τ_S *values, the authors should clearly state the fitting parameters employed. Ideally, an independent magneto-optical measurement (e.g., magnetic circular dichroism or magneto-PL) should be performed to calibrate the exciton g-factor. The current simplified treatment of the Hanle curve fitting warrants further justification.*

Our Response: We have carried out magnetic circularly polarized luminescence (MCPL) measurements to experimentally determine the effective Landé g-factors in Cs(PbMgZnCd)Br_3 and $CsPbBr_3$. As shown in **Figure R2**, the effective g-factors are extracted by the linear fittings of MCPL to be ~1.30 for Cs(PbMgZnCd)Br_3 and ~1.22 for $CsPbBr_3$, which are very close to the values in previous studies (Wang, et al., *Nat. Commun.* **2019**, *10*, 129). Cs(PbMgZnCd)Br_3 should be regarded as nanosized $CsPbBr_3$ domains stabilized by Cs(MgZnCd)Br_3, where Mg/Zn/Cd do not participate in optical transitions or spin-orbit coupling in $CsPbBr_3$.

Accordingly, we have added **Figure R2** as Figure S29 in the revised version. Using these experimentally obtained g-factor values, we have re-fitted the optical Hanle curves and updated the spin lifetimes (Figure 5d) in the revised manuscript.

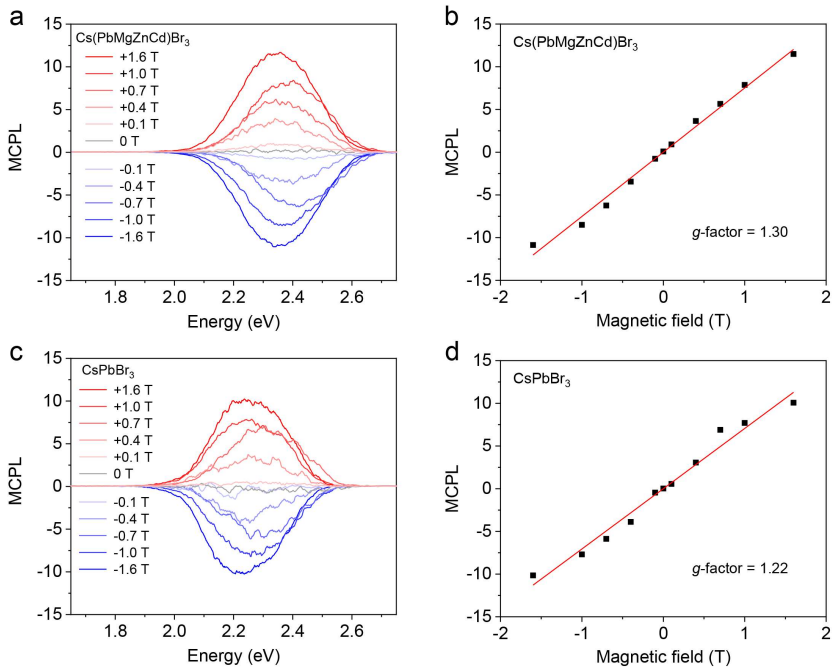

Figure R2. MCPL spectra of (a) $Cs(PbMgZnCd)Br_3$ and (c) $CsPbBr_3$ nanocrystal films. The magnetic field dependence of MCPL, from which the g-factor for the excitons in (b) $Cs(PbMgZnCd)Br_3$ and (d) $CsPbBr_3$ has been extracted.

4. A central conclusion of this work is the unique advantage of synergistic high-entropy doping (simultaneous incorporation of Mg, Zn, and Cd) in enhancing lattice distortion and prolonging τs. However, the experimental comparison is limited solely to undoped $CsPbBr_3$ versus $Cs(PbMgZnCd)Br_3$. Crucial control experiments involving single-metal doping (e.g., $CsPb_{1-x}Mg_xBr_3$) or binary doping at comparable total substitution levels are absent. While the authors note the difficulty of high-level single-metal doping, control samples prepared within the achievable doping limits would be highly valuable to confirm the necessity of the high-entropy configuration and to rule out simple additive effects of the individual dopants. The inclusion of such comparative data, or an extended discussion comparing the present results with existing literature on single-dopant τ_s values, would substantially strengthen the manuscript's claims.

Our Response: The large difference in ionic sizes between Pb and Mg/Zn/Cd make it theoretically impossible for single-metal substitution in the $CsPbBr_3$ perovskite, as the

structural stability of perovskites is evaluated using the Goldschmidt tolerance factor (refer to Bartel, et al., *Sci. Adv.* **2019**, *5*, eaav0693). Experimentally, we have attempted single-metal doping and binary doping controls, but could not synthesize perovskite nanocrystals at a reasonable doping level. Taking $CsPb_{1-x}Mg_xBr_3$ as a typical example, we measured only a trace amount of Mg dopant in the "single-metal doping" $CsPbBr_3$, where x is ~0.012 according to inductively coupled plasma analysis. This Mg-doped control sample shows nearly identical PL spectrum, PL lifetime and spin relaxation time compared to pristine $CsPbBr_3$, as shown in **Figure R3**. It indicates that the changes of photo-physical and spin-physical properties in $Cs(PbMgZnCd)Br_3$ cannot be due to simple additive effects of individual dopants, since these non-magnetic dopants do not participate in optical transitions or spin interactions in $CsPbBr_3$.

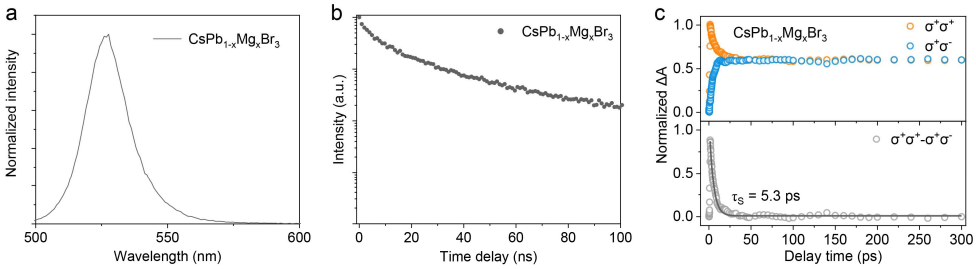

Figure R3. (a) PL spectra, (b) PL lifetime and (c) spin relaxation time measurements of $CsPb_{1-x}Mg_xBr_3$ nanocrystals.

Accordingly, we have added **Figure R3** as Figure S25 in the revised version. We have also clarified that the strong lattice distortion and prolonged spin relaxation in $Cs(PbMgZnCd)Br_3$ cannot be experimentally achieved in single-metal or binary doping samples, as they cannot be prepared at comparable total substitution levels.

5. The authors demonstrate a high degree of circular polarization (~25.8%) in amplified spontaneous emission (ASE) at room temperature and showcase multi-level optical write-in/read-out. This is a highlight of the work. However, the verification of the temporal and thermal stability of this polarized ASE, as well as its reproducibility, is rather limited (only briefly mentioned in relation to Figure S34). Furthermore, the high polarization is achieved under femtosecond pulsed excitation; it remains unclear

whether similar performance can be sustained under continuous-wave optical pumping or, ultimately, electrical injection, which is more relevant for practical device applications. The authors are encouraged to provide additional data on the evolution of ASE circular polarization over extended operation times (minutes to hours) and thermal cycling. A preliminary discussion or outlook regarding the potential performance under continuous excitation would enhance the technological relevance of these findings.

Our Response: We have measured the temporal stability of circularly polarized ASE from Cs(PbMgZnCd)Br_3, as shown in **Figure R4**. The σ^+ and σ^- ASE intensities show simultaneously an obvious decrease after 10 hours due to the partial degradation of samples, while the corresponding ASE circular polarization remains over ~20%. All the above experiments are carried out at room temperature, and the ASE polarization is reproducible during thermal cycling between room and cryogenic temperatures. In addition, we have tried CW optical pumping and observed no ASE signal at high excitation power. Electrically injected lasing is indeed appealing but beyond the scope of present work. We definitely agree that both CW excitation and electrical injection warrant future studies, as they are essentially important for the practical applications of spin-polarized lasers based on perovskite materials (Qin, et al., *Nature* **2020**, *585*, 53-57; Zou, et al., *Nature* **2025**, *645*, 369-374; added as refs. 57 and 58).

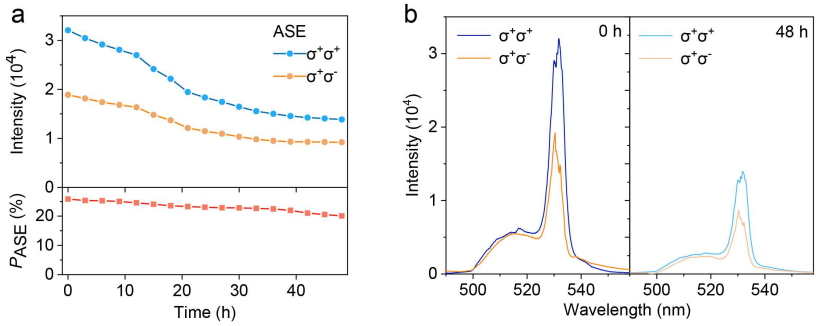

Figure R4. (a) Time-dependent plots of σ^+ and σ^- ASE intensities over 48 h under σ^+ pump and corresponding P values from Cs(PbMgZnCd)Br_3. (b) ASE spectra at 0 h and 48 h.

Accordingly, we have replaced Figure S36 with **Figure R4** in the revised version, and added a preliminary outlook on CW pumping and electric injection in Discussion.